Supporting Information for

Interface Effect on Electronic and Optical Properties of Antimonene/GaAs van der Waals Heterostructures

Ning Wang, [†] *Dan Cao,*[†,*] *Jun Wang,* [‡] *Pei Liang,* [‡] *Xiaoshuang Chen,* [§] *and Haibo Shu*[‡,*]

[†]College of Science and [‡]College of Optical and Electronic Technology, China Jiliang University, 310018 Hangzhou, China
[§]National Laboratory for Infrared Physics, Shanghai Institute of Technical Physics, Chinese Academy of Science, 200083 Shanghai, China

[*]Corresponding author. Dan Cao, E-mail: caodan@cjlu.edu.cn, Phone: 86-0571-86835756; Haibo Shu, E-mail: shu123hb@gmail.com, Phone: 86-0571-86875622;

S1. Geometries and Stability of Sb/GaAs heterostructures

The Sb/GaAs heterostructures are created by putting the Sb monolayer on perfect, reconstructed, and hydrogenated GaAs(111) surfaces, respectively. To faciliated our description, the Sb monolayer on perfect, reconstructed, hydrogenated GaAs(111)A surface are denoted by SGA-P, SGA-R, and SGA-H, respectively, and the Sb monolayer on perfect, reconstructed, hydrogenated GaAs(111)B surface are denoted by SGB-P, SGB-R, and SGB-H, respectively. For all GaAs(111) surfaces, there are three high-symmetry standing sites (A, B, and C shown in Fig. S1a). Therefore, the buckling Sb monolayer on each GaAs(111) surface will have six potential interfacial configurations. Taking SGA-P as an example, six potential interfacial configurations have been indicated in Fig. S1b. For each Sb/GaAs heterostructure, the most stable interfacial configuration is achieved by the energy comparision. A shown in Fig. S2a, it shows relative energies (ΔE) of various interfacial configurations in six Sb/GaAs heterostructures with respect to the lowest-energy configuration. The most stable atomic configurations of six Sb/GaAs heterostructures have been shown in Fig. S2b.

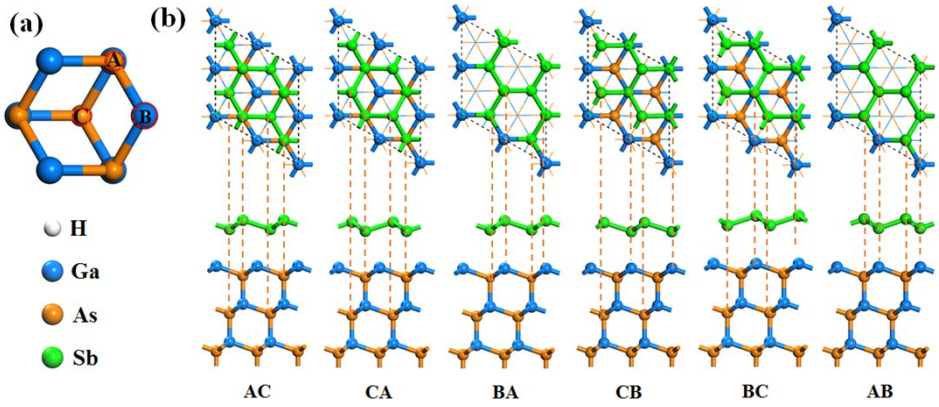

Fig. S1 (a) Top projection view of GaAs(111)A surface, where A, B and C denote three possible standing sites for the Sb atom in buckling Sb monolayer. (b) Six potential configurations for the Sb monolayer on GaAs(111)A clean surface.

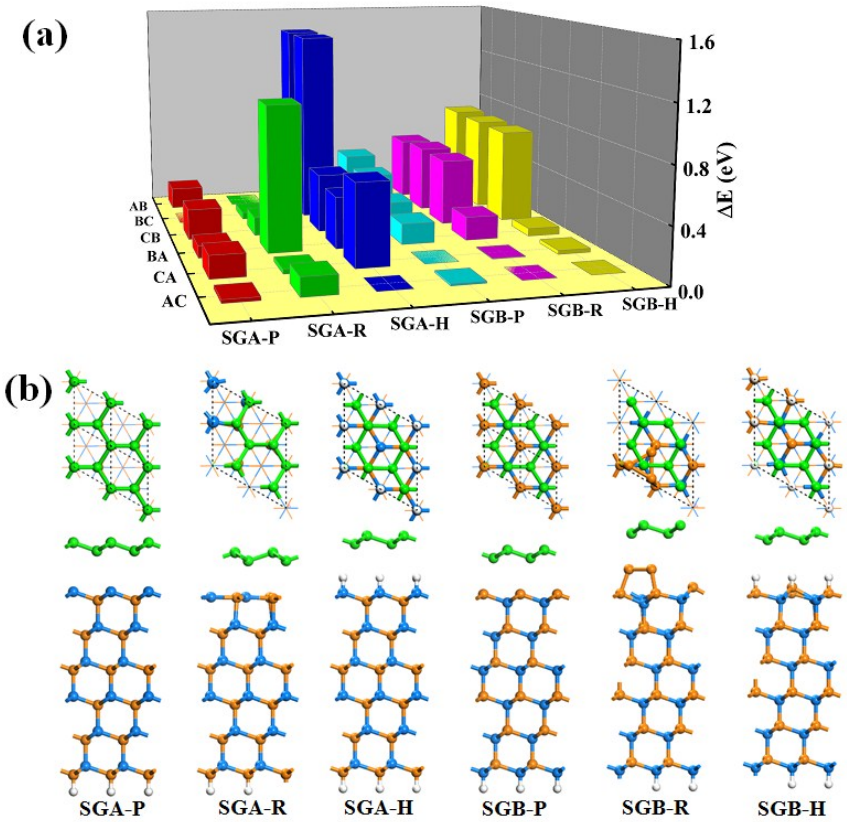

Fig. S2 (a) The relative energies of various potential interfacial configurations with respect to the lowest-energy configuration in six Sb/GaAs heterostructures. (b) Top and side views of the most stable interfacial configurations in six Sb/GaAs heterostructures.

S2. Band structures and interfacial states of perfect Sb/GaAs heterostructures

Fig. S3 shows band structures of perfect Sb/GaAs heterostructures (i.e., SGA-P and SGB-P). It can be found that there is a band across the Fermi level in both of two heterostructures, indicating a metallic characteritic. The charge-density isosurfaces indicate that the mid-gap states mainly localized at the interface of SGA-P and SGB-P heterostructures. It is a well-known fact that perfect GaAs(111) polar surfaces are unstable due to the existence of surface states, introducing the Sb monolayer cannot eliminate the surface states of GaAs(111) clean surfaces, resulting in the localization of electronic states at the interface of heterostructures.

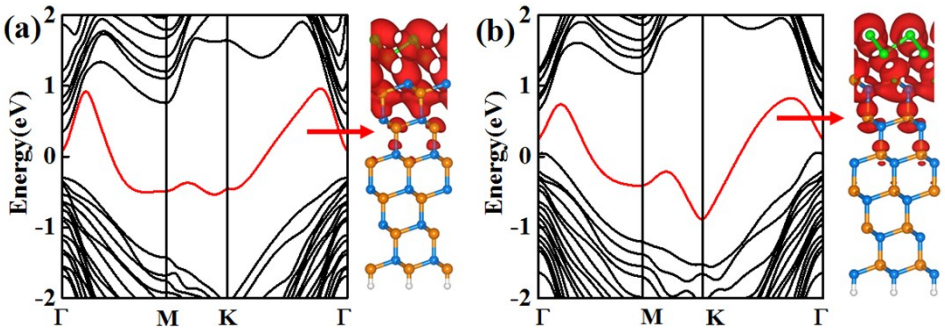

Fig. S3 Band structures and charge-density distribution of mid-gap states in (a) SGA-P and (b) SGB-P heterostructures. The Fermi level is shifted to zero. The mid gap states in band structures are colored in red.

S3. Band structure of a Sb monolayer

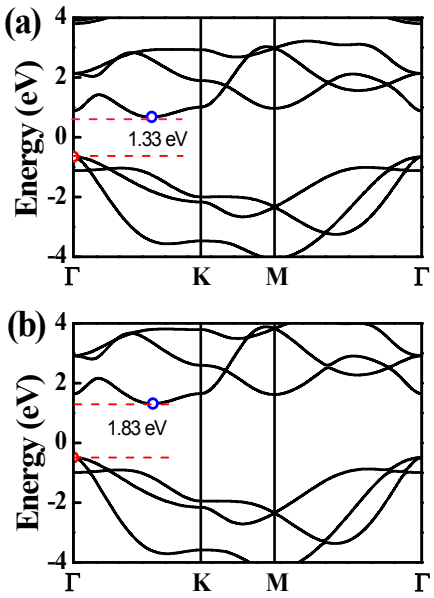

Fig. S4 Electronic band structure of Sb monolayer calculated using (a) PBE functional and (b) HSE06 function. Fermi level is shifted to zero. The band-gap values have been indicated in band structures.

S4. Density of states of Sb/GaAs heterostructures

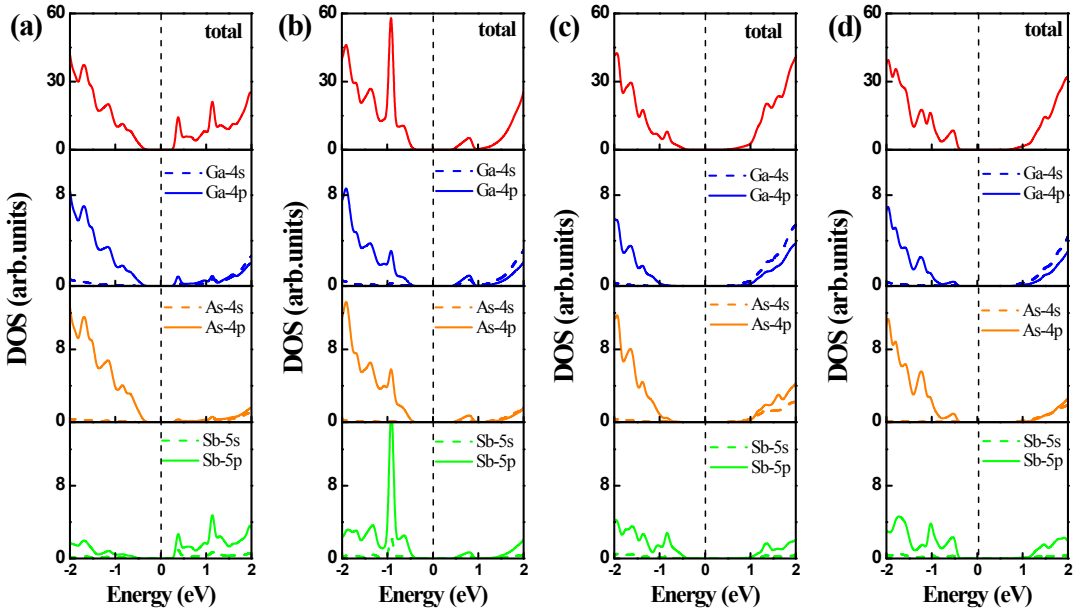

Fig. S5 Total and partial density of states (DOS) of four Sb/GaAs heterostructures. The DOS for (a) SGA-R, (b) SGA-H, (c) SGB-R, and (d) SGB-H. The vertical dash lines denote the position of Fermi level.